

Application of gene expression programming for modelling bearing capacity of aggregate pier reinforced clay

Ali Reza Ghanizadeh ^{a,*}, Farzad Safi Jahanshahi ^a and Seyed Saber Naserlavi ^a

^a Department of Civil Engineering, Sirjan University of Technology, Sirjan, Iran.

Article History:

Received: 17 July 2022.

Revised: 09 November 2023.

Accepted: 13 January 2024.

ABSTRACT

Utilizing the aggregate piers is one of the methods to improve and increase the bearing capacity of soft soils. The ultimate bearing capacity of these piers is affected by parameters such as the physical properties of the piers, structural conditions, the embedment depth and replacement ratio of piers, which complicates the estimation of bearing capacity. In this study, the Gene Expression Programming method was used for the prediction of the ultimate bearing capacity of clay soils reinforced with aggregate piers. For this purpose, two different models were developed, of which the first model (GEP2) utilized two input variables, the undrained shear strength of clay (S_u) and replacement ratio (a_r), while the second model (GEP4) used four input variables including the undrained shear strength of clay (S_u), replacement ratio (a_r), slenderness ratio (S_r), and embedment depth of piers (d_i). The coefficient of determination of the GEP2 model, and the GEP4 model is 0.921 and 0.942, respectively. Besides, comparing the GEP4 model of this research with the developed models of previous studies confirms the superior performance of the GEP4 model, considering both the accuracy and number of input parameters. The results of sensitivity analysis showed that the undrained shear strength of clay (S_u), replacement ratio (a_r), slenderness ratio (S_r), and embedment depth of piers (d_i) have the highest impact on the prediction of bearing capacity, respectively. Furthermore, the parametric analysis demonstrated that increasing the S_u , a_r , S_r , and d_i would improve the bearing capacity of the aggregate piers reinforced clay.

Keywords: *Aggregate piers, Bearing capacity, Clay soil, Gene expression programming.*

1. Introduction

Soft soils, including clay and slit, have low strength and high compressibility. Hence, soil improvements are required before constructing engineering structures on soft soils. There are various methods for soil improvement, including soil stabilization, pre-loading, and deep replacement. In the deep replacement method, the desired soil is excavated to a relatively large depth; afterward, it is replaced and filled with high-quality materials in the form of a series of columns. These supports, along with the surrounding soil, form a composite foundation with an increased bearing capacity to withstand horizontal and vertical loads [1, 2]. Besides being useful, cost-efficient, and environmentally friendly, the deep replacement method helps to reduce overall and differential settlement and stabilize slopes. Some of the deep replacement methods are vibro-replacement, vibro-displacement, vibro-concrete column, controlled modulus column, sand compaction column, encased granular column, aggregate pier, dynamic replacement, and sand columns [2]. The deep replacement methods can bring benefits such as increasing soil bearing capacity, increasing compaction, increasing liquefaction resistance, reducing settlement, providing lateral support, and accelerating consolidation [3–7].

Recently, the aggregate pier method has been widely evaluated and used to increase bearing capacity, reduce settlement, and horizontal displacement under the foundation [8–12]. In general, aggregate piers consist of four categories, including the single isolated pier, the intermediate single pier, the intermediate group of piers, and the group of piers [13]. Failure modes of aggregate piers consist of bulging, punching, and shear failure, which are depicted in Figure (1). The

bulging failure is most likely to happen in aggregate piers constructed in clay, and is usually observed at the upper part of the column (3-2 times the diameter of the column) [2]. The failure modes of stone columns or aggregate piers depend on the column type (based on its length and diameter), the type of loading on the column, and soil strength [14].

According to Figure (1a), the zone highlighted in red has the highest chance of bulging failure. If floating aggregate piers are placed in soft soil (Figure 1b), the aggregate piers would be unstable due to punching failure, which happens before bulging failure, especially if the length of aggregate piers is less than 3-2 times their diameter [15].

Since the early 1970s, several techniques have been proposed to predict the bearing capacity of the aggregate pier, including methods based on plasticity and elasticity theory [16], cavity expansion theory [17, 18], numerical methods [19–22], empirical methods [23–26], and soft computing-based methods [27–29]. Numerous field and laboratory experiments have been performed to investigate the failure mechanism and also to evaluate the bearing capacity of aggregate piers [30–33]. Ambily and Gandhi performed a high-precision experiment on the behavior of a single and a group of stone columns. Subsequently, they compared the results with those obtained from the finite element method [34]. Hanna et al. presented a finite element (FE) model for evaluating the performance of stone column in soft soils [35]. Mohanty and Samantha, apart from investigating the behavior of aggregate piers in the laboratory, proposed a numerical method to predict the bearing capacity [36]. The 3D FE model proposed by Algin and Gumus

* Corresponding author: Tel./Fax: +98-9126495932, E-mail address: ghanizadeh@sirjantech.ac.ir (A.R. Ghanizadeh).

considered the effect of parameters during the construction and installation of stone columns [37]. Etezad et al. developed a numerical analysis method to estimate the bearing capacity of soft soils reinforced with stone columns. They compared its results with laboratory findings to evaluate this model [38]. Naseer et al. used numerical and laboratory investigations to evaluate the effect of sand columns in soft clay soils [39]. Also, Stuedlein and Holtz compared the accuracy of existing analytical models for estimating the bearing capacity of aggregate piers by evaluating 30 loading experiments in various field conditions. They demonstrated that the existing models have a wide range of biases and errors. They concluded that these models are usually unsuitable for practical designs due to their wide range of mistakes. Hence, a modified model is required to determine the bearing capacity [13].

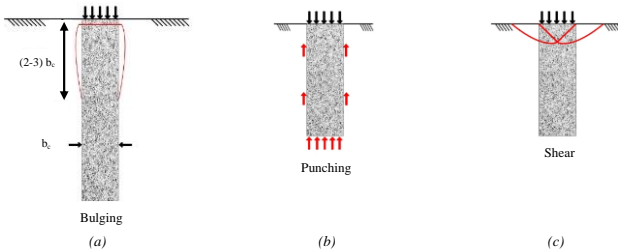


Figure 1. The failure modes for stone columns and aggregate piers.

In recent decades, employing soft-computing methods, including Artificial Neural Networks (ANNs) and Adaptive Neuro-Fuzzy Inference Systems (ANFIS), has been popularized in civil engineering due to their capability and adaptability [40–48]. Many researchers used these techniques to predict axial and lateral bearing capacity, pull-out resistance, and efficiency of piles [13, 33, 39, 49–56]. Among these studies, Goh evaluated the friction capacity of driven piles by the ANN [49]. Fattah et al. used a regression model to predict stone columns' bearing capacity (SCBC) [33]. In 2018, Das and Dey employed the ANN to predict the SCBC. They showed that ANN has superior predictive capability compared to previously established theories [52]. Dey and Debnath used the Support Vector Regression (SVR) method to assess the ultimate bearing capacity of a stone column reinforced with geogrid. They also compared the SVR with the ANFIS method and concluded that the SVR model outperforms the ANFIS model [53]. Ardakani et al. predicted the SCBC installed in the clay containing slit soil by the back-propagation ANN and optimized ANN using Imperialist Competitive Algorithm (ANN-ICA). This study confirms the superiority of ANN-ICA compared to back-propagation ANN methods [54]. Although the neural network method has been used to predict the bearing capacity, it is referred to as a black box model due to the complexity of the model and matrix calculations [29]. Ghanizadeh et al. employed Multivariate Adaptive Regression Spline (MARS) optimized by a metaheuristic algorithm to build a model for predicting the bearing capacity of geogrid reinforced stone columns [27].

Dehghan banadaki used ANFIS to predict the SCBC in soft soils [55]. According to the satisfactory accuracy of the proposed ANFIS, they suggested this model to design floating column-like elements for subgrade improvement. Type-2 Fuzzy Set (T2FS) was used by Das and Dey in 2022 to estimate SCBC. In this study, T2FS outperformed ANN and ANFIS models for the prediction of SCBC [56]. Stuedlein and Holtz developed a model based on the multiple linear regression method for estimating the bearing capacity of aggregate piers. The input variables in this study were assumed to be the slenderness ratio (S_r), replacement ratio (a_r), embedment depth (d_f), and undrained shear strength of clay (S_u). Equation (1) was proposed for estimating the bearing capacity [13]. It should be noted that the slenderness ratio is the ratio of aggregate pier length to its diameter ($S_r = L_p / d_p$).

$$\ln(q_{ult}) = 4.756 + 0.013 \times S_r + 1.914 \times a_r + 0.07 \times d_f \times S_r - 13.71 \times \left(\frac{S_u}{a_r}\right)^{-1} + 0.005 \times \frac{S_u}{a_r} \quad (1)$$

Bong et al. used the multiple linear regression method and deep

neural network to determine the bearing capacity of the aggregate piers [29]. According to Equation (2), four independent variables, including undrained shear strength of clay (S_u), replacement ratio (a_r), embedment depth (d_f), and slenderness ratio (S_r), were used:

$$q_{ult} = 67.8 \times \frac{1}{a_r} + 169.3 \times \sqrt{S_u \times a_r} + 271.4 \times d_f^2 - 626.5 \times \frac{1}{S_r} - 256.8 \quad (2)$$

It should be considered that in Equation (2), a_r is a ratio and not a percentage. R^2 of this model was calculated as 0.93. Also, the R^2 of the deep neural network method was 0.92 [29]. Dadhich et al. also predicted the bearing capacity of aggregate piers by the linear regression, support vector machine, random forest, and ANN methods [28]. Equation (3) was suggested for the prediction of the bearing capacity of the stone columns:

$$q_u = 11.74 \times S_u + 4.69 \times a_r + 19.86 \times B_f + 279.56 \times d_f + 297.17 \times d_p + 2.72 \times L_p + 14.88 \times S_r - 642.43 \quad (3)$$

In this equation, the undrained shear strength of clay (S_u), replacement ratio (a_r), diameter or width of the column (B_f), embedment depth (d_f), diameter of the aggregate pier (d_p), length of the aggregate pier (L_p), and slenderness ratio (S_r) were used as input variables. The coefficient of determination (R^2) for Equation (3) and the developed support-vector regression (SVR), random forest regression (RFR), and ANN models were 0.901, 0.88, 0.98, and 0.89, respectively [28].

In previous studies, various methods were employed, including ANN, ANFIS, SVR, RFR, linear and non-linear regression methods, to predict the bearing capacity of the aggregate piers reinforced clay. But, each of these methods has its drawbacks. The ANN cannot provide a simple equation to calculate the bearing capacity due to being a black-box method. Besides, it is unsuitable for modelling when the dataset has a small number of records and might result in over-fitting. In developing multiple non-linear models, considering that the shape of the model is presumed and is not fully definable, the best and most accurate equation for the prediction of the bearing capacity is not achievable.

In this study, the Gene Expression Programming (GEP) method is employed to predict the ultimate bearing capacity of clay soil reinforced by aggregate piers. In the GEP method, the accuracy of the developed model is increased by precisely determining the non-linear equation. This method is also suitable for a small amount of data. Besides, in this study, two different models based on GEP have been developed. One is able to estimate the ultimate bearing capacity by two variables (GEP2), and the other uses four variables to do so (GEP4). These two models may be used depending on the available information and design details. After sensitivity analysis and determining the importance degree of each input parameter, the parametric analysis was performed to evaluate the effect of each input variables on the bearing capacity based on the optimal model (GEP4). Also, the accuracy of the optimal developed model in this research was compared with the accuracy of previously proposed models.

2. Methods

2.1. Gene Expression Programming

GEP is an evolutionary algorithm that, like genetic programming and genetic algorithm, relies on a population. This population evolves based on a fitness criterion and one or multiple genetic operators [57]. The GEP consists of linear chromosomes with a constant length, and expression trees with various shapes and lengths. These features are inspired by the genetic algorithm and genetic programming, respectively [58]. The main steps of the GEP are depicted in Figure (2).

As can be seen in Figure (2), this process is repeated until a proper answer is achieved. All the GEP genes have the same length, but they can code expression trees (ET) with different shapes and lengths. A chromosome is formed, with the help of linking functions, by placing different genes next to each other. The ET, depicted in Figure (3) for Equation (4), presents various factors such as functions, constants, operators, and variables.

$$[a + (a + b)] - [a - \sqrt{b}] \quad (4)$$

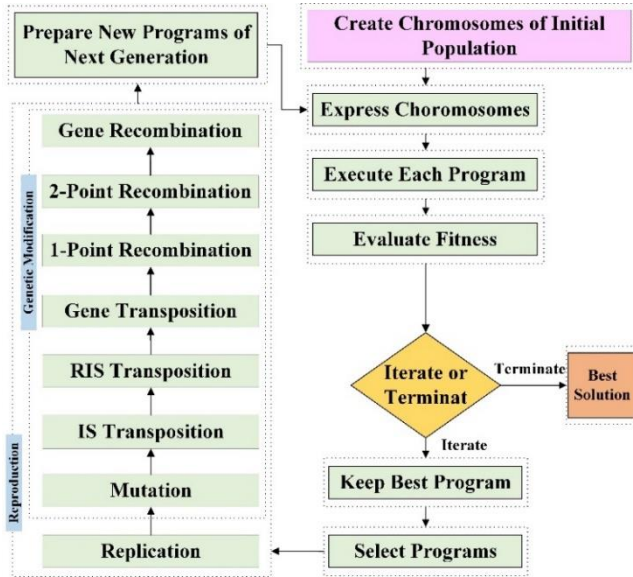


Figure 2. The flowchart for building a GEP model [59].

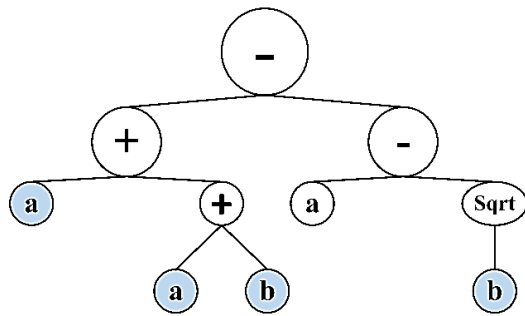


Figure 3. The expression tree of a chromosome

Figure (4a) depicts a crossover operator when, to improve fitness expansion, a random branch from the parent tree is replaced by another random branch or element. Therefore, two offspring, each inheriting genetic data from either of the parents, are generated from this crossover operator. Figure (4b) presents a mutation operator that happened by replacing a random branch in a node of the parent tree with another newly generated branch or element [60].

Previous research has shown the advantages of the GEP method over classical regression methods [61, 62]. In classical regression methods, the function is defined before analysis, whereas in GEP, no predefined function is considered. Therefore, GEP performs better in modelling and extracting equation from empirical studies with multiple variables compared to regression techniques [63, 64]. To achieve maximum accuracy, no exact method is available to attain the optimal model with a combination of parameters, and due to its complexity, the duration of the modelling process increases.

In this study, different values of effective variables were examined in GEP to achieve higher efficiency and less complex fittings. First, to maximize the accuracy of each model, the least possible number of gene parameters was utilized, and then, to expand the model, a combination of input variables was used. The linking function used in this GEP was addition. A problem was solved by choosing a single-gene chromosome and adding to its head length. However, the number of genes can be increased, and if the number is significant, a function can be chosen to link the branches of expression trees (sub-expression trees (sub-Ets)) [65]. Increasing input variables, the number of genes, and head size would make the model more complex. The complexity can also increase by the addition of new generations for better fitness [66]. There are five main steps when using GEP; three define the search space algorithm,

and the last two determine the quality and speed of the search. These steps consist of:

- 1- Choosing the fitness function. In this study, the fitness function (F_i) is considered as the mean square error (MSE).

$$f = \frac{1}{n} \sum_{j=1}^n (\hat{y}_j - y_j)^2 \quad (5)$$

In this equation, \hat{y}_j is the predicted value for data point "j" (where the total number of data points is n), and y_j is the measured value for the data point "j".

- 2- Choosing the terminal (T) and functions (F) for the chromosome generation. Here, the terminal consists of independent variables, and the function set comprises four arithmetic operators (+, -, *, /), as well as some fundamental mathematical operators (such as square root and x^2). The weight of all functions is considered as 1.
- 3- Choosing the architecture of the chromosomes, including the number of genes and head size. In this study, between 3 and 7 genes were selected with a head size of 4 to 7, and at the end, the optimum amounts of genes and head size were determined by the results of training and testing sets.
- 4- Choosing the linking function to connect sub-ETs. In this research, after examining different functions and evaluating their accuracy, the "addition" function has been used.
- 5- Utilizing a combination of all genetic operators, consisting of selection, crossover, and mutation.

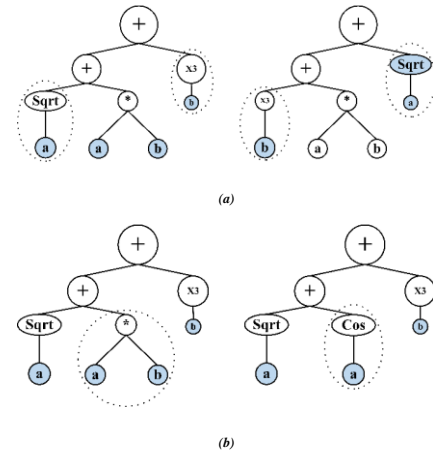


Figure 4: The expression trees in the GEP, a) Crossover operator, b) Mutation operator

2.2. Evaluation of the Model Accuracy

Several indexes were used in this study to evaluate the performance and accuracy of the proposed GEP models based on the training and testing data, including the coefficient of determination (R^2), root-mean-square deviation (RMSE), mean absolute error (MAE), root relative squared error (RRSE), and relative absolute error (RAE). The following equations show relations for these indexes

$$R^2 = \frac{(n \sum t_i o_i - \sum t_i \sum o_i)^2}{(n \sum t_i^2 - (\sum t_i)^2)(n \sum o_i^2 - (\sum o_i)^2)} \quad (6)$$

$$RMSE = \sqrt{\frac{1}{n} \sum_{i=1}^n (t_i - o_i)^2} \quad (7)$$

$$MAE = \frac{1}{n} \sum_{i=1}^n |t_i - o_i| \quad (8)$$

$$RRSE = \sqrt{\frac{\sum_i (t_i - o_i)^2}{\sum_i (t_i - (1/n) \sum_i t_i)^2}} \quad (9)$$

$$RAE = \frac{\sum_i |t_i - o_i|}{\sum_i |t_i - (1/n) \sum_i t_i|} \quad (10)$$

In the equations mentioned above, the measured value (real), model output value, and the number of all data points are presented as t , o , and n , respectively.

3. Experimental Dataset

In this study, 37 bearing capacity data points determined by field loading tests were used to develop the GEP models, including 30 data collected by [13] and seven data collected by [67]. In fact, 30 data points collected by [13] are from different resources. The experimental dataset is provided in Table 1. As shown in Table 1, piers configuration, piers dimensions, shear strength of soil for data points in [67] are consistent with these values in [68-75]. On the other hand, the high accuracy of models developed in the current research, as well as previous researches, confirms the consistency of data points gathered from different sources. The dataset consisted of 27 circular foundations and 10 square foundations. The length of the aggregate piers (L_p) was in the range of 2.3 to 14 meters, the diameter (d_p) was in the range of 30 to 100 centimeters, and the slenderness ratio (S_r) was from 2 to 26.67. Besides, the replacement ratio (a_r) was between 16% and 122 %. Drop ram, tamped, and vibrated methods were used to construct aggregate piers. Also, the undrained shear strength of soil (S_u) was in the range of 12 to 100 kPa. Further details regarding the field and laboratory experiments are presented in the two references.

Bong et al. demonstrated that the bearing capacity of aggregate piers reinforced clay is affected by four variables, including the undrained

shear strength of soil (S_u), replacement ratio (a_r), embedment depth (d_f), and slenderness ratio (S_r) [29]. These four variables are employed in this study to predict the bearing capacity. The statistical characteristics of the dataset are presented in Table (2).

The Pearson Correlation Coefficients of different variables are depicted in Figure (5). It is observed that the bearing capacity is mostly correlated with the undrained shear strength of soil, replacement ratio, embedment depth, and slenderness ratio, in that order. Two different hypothetical conditions are considered for the development of the GEP models, and the results are compared, including:

1. Considering two variables, S_u and a_r , as independent variables (GEP2 model)
2. Considering four variables, S_u , a_r , d_f , and S_r as independent variables (GEP4 model)

Variables S_u and a_r were chosen due to the relatively high correlation of these two variables with the bearing capacity. The investigation through the construction of additional GEP models revealed that removing each of these two parameters in the modelling procedure will significantly reduce the modeling accuracy.

Table 1. Experimental dataset.

Footing Shape	Compaction Method	S_u (kPa)	a_r (%)	d_f (m)	d_p (m)	L_p (m)	$S_r = L_p/d_p$	q_{ult} (kPa)	Pier Configuration	Reference
Circular	Drop ram	30	100	0	0.3	8	26.67	722	SP	[68]
Circular	Drop ram	30	44.4	0	0.3	8	26.67	396	ISP	[68]
Circular	Drop ram	30	25	0	0.3	8	26.67	559	ISP	[68]
Circular	Drop ram	30	16	0	0.3	8	26.67	482	ISP	[68]
Circular	Vibrated	12	46.8	0	1	5	5	189	IGP	[69]
Square	Vibrated	59	30.2	0	0.74	4.57	6.18	555	GP	[70]
Square	Vibrated	54	24.2	0	0.74	4.57	6.18	532	GP	[70]
Square	Vibrated	59	30.2	0	0.74	3.05	4.12	645	GP	[70]
Square	Tamped	75	30.2	0	0.76	4.57	6.01	624	GP	[70]
Square	Vibrated	65	30.2	0	0.74	4.57	6.18	615	GP	[70]
Circular	Vibrated	44	40.1	0.61	0.61	2.9	4.75	399	ISP	[71]
Circular	Vibrated	22	122	0	0.73	10	13.7	628	SP	[72]
Square	Vibrated	12	36	0	0.85	14	16.47	177	ISP	[73]
Square	Vibrated	12	36	0	0.85	14	16.47	252	ISP	[73]
Circular	Vibrated	12	100	0	0.85	14	16.47	378	SP	[73]
Circular	Rammed	100	100	0	0.61	3.05	5	1346	SP	[74]
Square	Rammed	30	34.6	0.46	0.76	2.33	3.07	338	GP	[75]
Square	Rammed	30	34.6	0.46	0.76	4.64	6.11	477	GP	[75]
Circular	Rammed	30	100	0.46	0.76	2.33	3.07	604	SP	[75]
Circular	Rammed	30	100	0.46	0.76	4.64	6.11	664	SP	[75]
Circular	Tamped	65	100	0.61	0.76	3.05	4.01	1096	SP	[70]
Circular	Tamped	69	100	0.61	0.76	3.05	4.01	1006	SP	[70]
Circular	Tamped	67	100	0.61	0.76	4.57	6.01	1132	SP	[70]
Circular	Tamped	70	100	0.61	0.76	4.57	6.01	1202	SP	[70]
Circular	Vibrated	57	95	0.61	0.74	3.05	4.12	1115	SP	[70]
Circular	Vibrated	61	100	0.61	0.76	3.05	4.01	1093	SP	[70]
Circular	Vibrated	63	88	0.61	0.71	3.05	4.3	1067	SP	[70]
Circular	Vibrated	61	95	0.61	0.74	4.57	6.18	1214	SP	[70]
Circular	Vibrated	53	95	0.61	0.74	4.57	6.18	1071	SP	[70]
Circular	Vibrated	52	95	0.61	0.74	4.57	6.18	1106	SP	[70]
Circular	Tamped	56	100	0.46	0.76	2.28	3	851	SP	[67]
Circular	Tamped	56	100	0.46	0.76	3.8	5	1244	SP	[67]
Circular	Tamped	49	100	0.46	0.76	1.52	2	823	SP	[67]
Circular	Tamped	49	100	0.46	0.76	2.28	3	697	SP	[67]
Circular	Tamped	49	100	0.46	0.76	3.04	4	813	SP	[67]
Circular	Tamped	49	100	0.46	0.76	3.8	5	888	SP	[67]
Square	Tamped	49	30.5	0.46	0.76	3.04	4	590	GP	[67]

Table 2. Statistical characteristics of the experimental dataset.

	S _u (kPa)	a _r (%)	d _f (m)	s _r	q _{ult} (kPa)
count	37	37	37	37	37
mean	47.05	72.41	0.32	8.34	745.68
std	20.29	33.98	0.27	7.42	325.02
min	12.00	16.00	0.00	2.00	177.00
25%	30.00	34.60	0.00	4.01	532.00
50%	49.00	95.00	0.46	6.01	664.00
75%	61.00	100.00	0.61	6.18	1071.00
max	100.00	122.00	0.61	26.67	1346.00

S_u: undrained shear strength of soil
a_r: replacement ratio
d_f: embedment depth
s_r: slenderness ratio
q_{ult}: bearing capacity

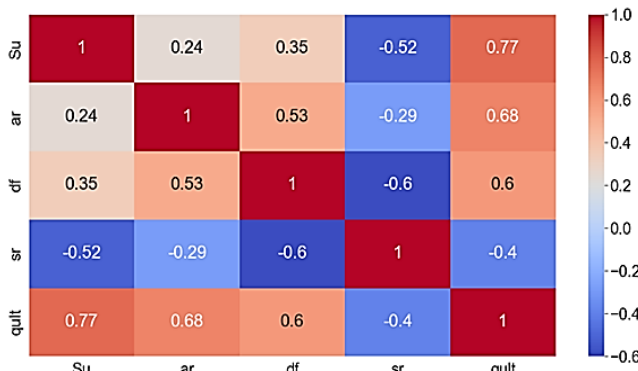


Figure 5. The Pearson Correlation Coefficient between dataset variables.

4. GEP Model Development

The GenXpro tool 5.0 software is used to develop the GEP models. The general setting to develop the model for predicting the bearing capacity of the aggregate piers reinforced clay is considered according to Table (3). It should be noted that the optimum values for these parameters are acquired by the trial and error method so that the under-fitting and over-fitting do not occur. The optimal number of genes and head size are 4 and 6 for the GEP4 model and 6 and 4 for the GEP2 model, respectively.

Table 3. The settings used to develop the GEP models.

Parameter	Value
General	
Chromosomes	150
Genes	4 and 6
Head size	6 and 4
Linking Function	Addition
Genetic Operators	
Mutation rate	0.00138
Inversion rate	0.00546
IS transposition rate	0.00546
RIS transposition rate	0.00546
One-point recombination rate	0.00277
Two-point recombination rate	0.00277
Gene recombination rate	0.00277
Gene transposition rate	0.00277
Numerical constants	
Constants per gene	10
Data type	Floating point
Lower band	-30
Upper band	30

The equation developed by the GEP method using two input variables, S_u and a_r (GEP2 model), and also using four input variables, S_u, a_r, d_f, and s_r (GEP4 model), are presented in Equation (11) and (12), respectively. The expression trees of the GEP2 and GEP4 models are depicted in Figures (6) and (7), respectively. In these figures, “C” denotes a constant value, “d” denotes an input variable, 3Rt(x) denotes $\sqrt[3]{x}$, Sqrt(x) denotes x², NOT(x) denotes (1-x), and Neg(x) denotes (-x).

$$q_{ult} = 58.5053 \times (S_u - a_r)^{\frac{1}{3}} - \frac{41.116}{24.7968 - a_r} + \sqrt{a_r^2 \times S_u} - (39.5333) + ((a_r - S_u)^2 \times (2411.7401))^{\frac{1}{3}} \tag{11}$$

$$q_{ult} = ((S_r + a_r) \times (S_r))^{\frac{2}{3}} + ((d_f \times (S_r + 0.4146)) \times (a_r - 42.7055)) + S_r \times (29.6817 - a_r)^{\frac{1}{3}} + (-45.6424 + 2S_u) + (3.3793 \times S_r) + \frac{23.5620}{17.4048 - 0.180053a_r} + ((2S_u)^{\frac{1}{3}} \times (S_u + a_r)) \tag{12}$$

The performance indexes for the two developed GEP models are given separately for the training and testing datasets in Table (4). It is observed that the coefficient of determination (R²) values for all data in the two models, GEP2 and GEP4, are 0.927 and 0.942, respectively. The root mean square error (RMSE) for GEP2 and GEP4 models are 91.72 and 78.61, respectively. In other words, the accuracy of the model using four independent variables with regard to test data (RMSE=86.52) is higher compared to the model with two independent variables (RMSE=119.02). Furthermore, the performance indexes of the GEP4 model regarding training and testing sets are much closer than the performance indexes of the GEP2 model regarding the training and testing datasets, which indicates that the GEP2 model is overfitted compared to the GEP4 model. Although the GEP4 model is more complex compared to the GEP2, it is suggested to use this model to estimate the bearing capacity due to higher accuracy and reliability.

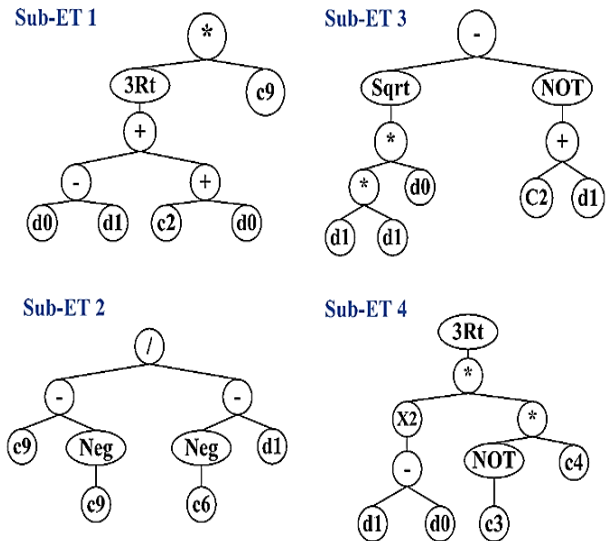


Figure 6. The expression trees for the GEP2 model.

The performance of the GEP2 and GEP4 models is depicted in Figures (8) and (9), respectively. The proximity of data points to the equality line indicates that both models have a good ability to predict the bearing capacity. The comparison between the measured bearing capacity and the bearing capacity predicted by the GEP2 and GEP4 models is depicted in Figures (10) and (11), respectively. The absolute relative error (ARE) is also depicted for each data in these figures. As can be seen, regarding the GEP2 model, four data points have an ARE of more than 20%, while the GEP4 model only has four data points with an ARE of more than 20%. Consequently, the GEP model with four

independent variables (GEP4) is more accurate at estimating the bearing capacity of aggregate piers reinforced clay.

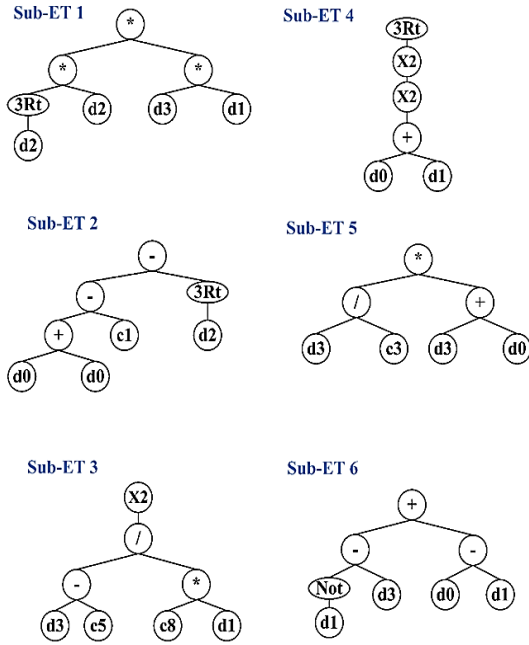
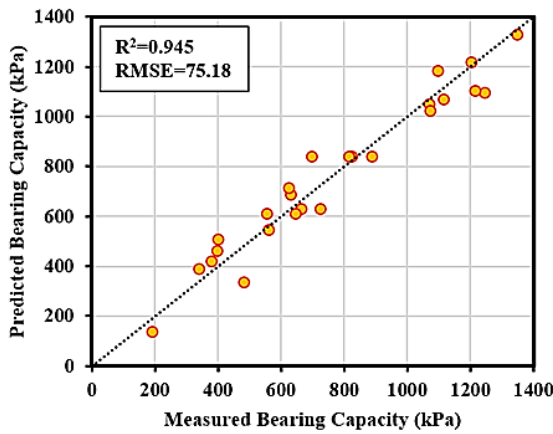
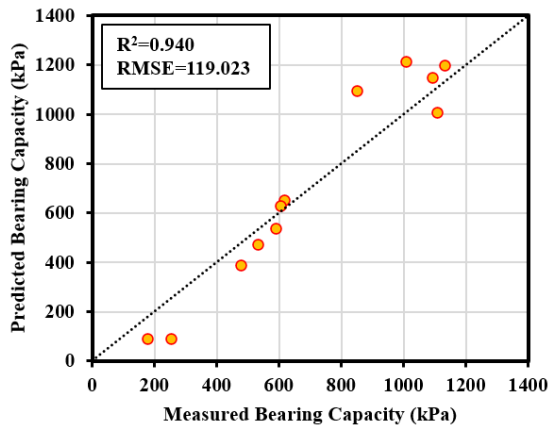


Figure 7. The expression trees for the GEP4 model.

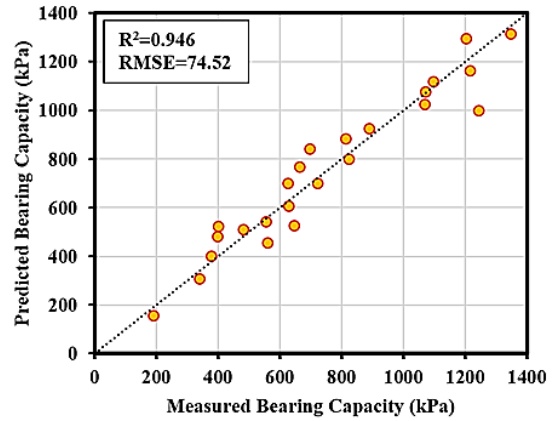


(a)

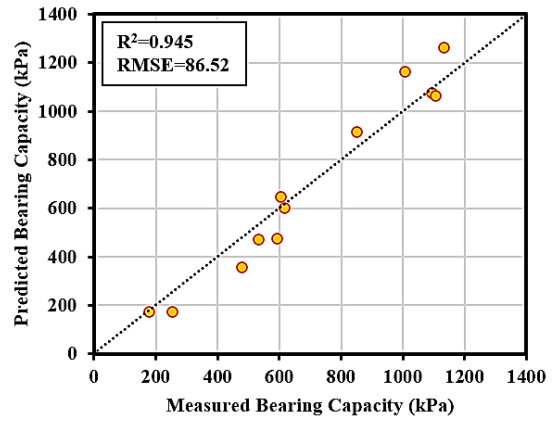


(b)

Figure 8: Performance of the GEP2 Model, a) Training dataset, b) Testing dataset.



(a)



(b)

Figure 9: Performance of the GEP4 Model, a) Training dataset, b) Testing dataset.

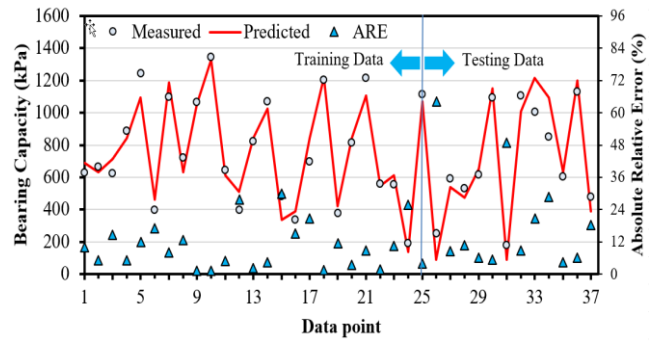


Figure 10. Comparison of the measured and the predicted bearing capacity using the GEP2 model.

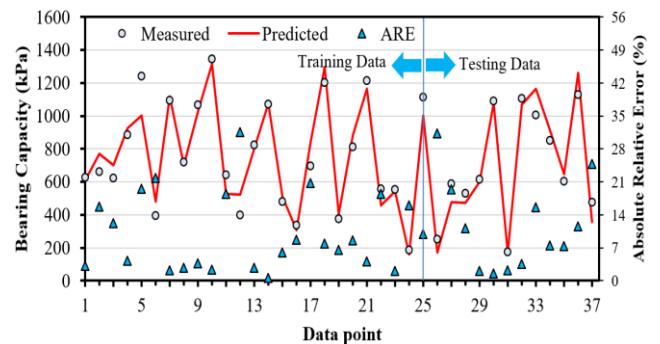


Figure 11. Comparison of the measured and the predicted bearing capacity using the GEP4 model.

5. Comparison with Previously Proposed Models

In this section, the accuracy of the optimal developed model, GEP4, is compared to other proposed models. For this comparison, models developed by Stuedlein & Holtz (2013), Bong et al. (2020), and Dadhich et al. (2021) were used to predict the bearing capacity of aggregate piers reinforced clay [13, 28, 29]. Among them, Dadhich et al., Bong et al., and Stuedlein and Holtz developed models for predicting the bearing capacity of the aggregate piers reinforced clay using seven, four, and four independent variables, respectively. The types of models, independent variables, and performance indicators of each model are presented in Table (5). For the DNN, ANN, SVM, and RFR models, performance indicators were extracted from the published papers, and for the MLR and MNR, the performance indicators were computed by authors based on the proposed regression models.

It is observed that the GEP4 model is more accurate compared to the MLR, MNR, DNN, SVM, and ANN models, and only the RFR model had better performance indexes than the GEP4 model. However, the RFR model is much more complex than the GEP4 model developed in this study, and Dadhich et al. [28] did not give details of the RFR model for use and implementation by engineers. Besides, the model presented in this study requires only four input variables, while the RFR model needs seven parameters to estimate the bearing capacity, and so it is more complicated. On the other hand, details of the ANN, SVM, and DNN models have not been provided, so engineers and researchers cannot use these models for further studies. The bearing capacities estimated by the MLR, MNR, and GEP4 models are depicted and compared in Figure 12. In this Figure, 20% error lines are represented as well. As can be seen, the GEP4 model has less dispersion compared to other presented models. Besides, the GEP4 model presented in this study has an error of less than 20% in most cases, while other models show higher errors, such that these models have an error of more than 300% in some data points. It is observed that the GEP4 model is more accurate compared to the MLR, MNR, DNN, SVM, and ANN models, and only the RFR model had better performance indexes than the GEP4 model. However, the RFR model is much more complex than the GEP4 model developed in this study, and Dadhich et al. [28] did not give details of the RFR model for use and implementation by engineers. Besides, the model presented in this study requires only four input variables, while the RFR model needs seven parameters to estimate the bearing capacity, and so it is more complicated. On the other hand, details of the ANN, SVM, and DNN models have not been provided, so engineers and researchers cannot use these models for further studies. The bearing capacities estimated by the MLR, MNR, and GEP4 models are depicted and compared in Figure 12. In this Figure, 20% error lines are represented as well. As can be seen, the GEP4 model has less dispersion compared to other presented models. Besides, the GEP4 model presented in this study has an error of less than 20% in most cases, while other models show higher errors, such that these models have an error of more than 300% in some data points.

6. Sensitivity analysis

It is necessary to perform various analyses on the developed model to validate the performance of the proposed models for new and unseen data [76]. The sensitivity analysis evaluates the degree of importance of the input parameters on the model output [77]. The method developed by Gandomi et al. and Javed et al. was used in this study for the sensitivity analysis [78, 79]. In this method, the effect of a single parameter on the output of the model is considered. The application of this method facilitates the evaluation of results and the extension of these results to real data [80]. Numerous researchers have used this method in their research [81, 82]. Equations (13) and (14) are used to evaluate the contribution of each input value to the output.

$$t_i = f_{\max}(q_i) - f_{\min}(q_i) \quad (13)$$

$$SA (\%) = \frac{T_i}{\sum_{i=1}^n T_j} \times 100 \quad (14)$$

In these equations, $f_{\max}(q_i)$ and $f_{\min}(q_i)$ are the minimum and maximum values of q_{ult} based on the i^{th} input domain, respectively, while the rest of the variables are considered constant and equal to their mean value. SA has a value between 0 and 100, which represents the contribution of each input variable to the bearing capacity evaluation (SA=100 means the highest contribution, and SA=0 represents the lowest) [83, 84]. The sensitivity analysis of the optimal model (GEP4) is depicted in Figure 13. As evident, the undrained shear strength of soil (S_u), replacement ratio (a_r), slenderness ratio (S_r), and embedment depth (d_f) had the highest contribution to the bearing capacity of the aggregate piers reinforced clay, in order.

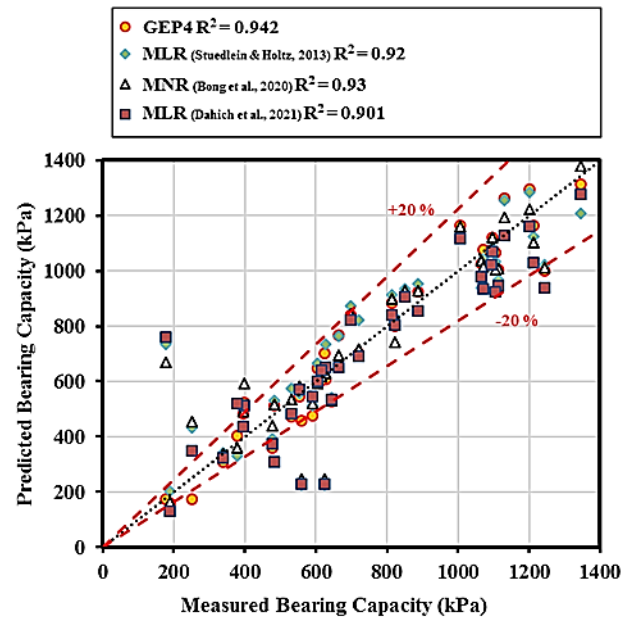


Figure 12. The comparison of accuracy for the MLR, MNR, and GEP models for predicting aggregate piers bearing capacity.

7. Parametric analysis

The parametric analysis (Figure 14) was performed to evaluate the effect of each variable on the bearing capacity. As presented in Figure 14, the bearing capacity increases if each input variable is increased. However, as observed, increasing the undrained shear strength of soil (S_u) has the highest effect, while the embedment depth (d_f) had the least effect on the bearing capacity.

It is also observed that the undrained shear strength of soil (S_u), slenderness ratio (S_r), and embedment depth (d_f) increased the bearing capacity linearly, while the replacement ratio (a_r) had a non-linear effect on the bearing capacity.

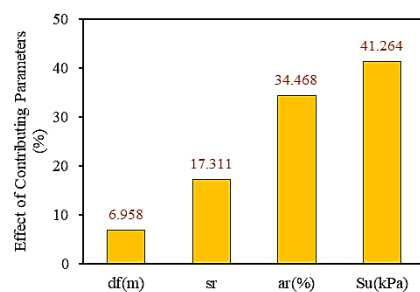


Figure 13. The sensitivity analysis for the GEP4 model.

Table 4. Statistical indexes for the GEP2 and GEP4 models.

Model	Training	Testing	Overall	Training	Testing	Overall
	GEP2			GEP4		
Input parameters	S_u, a_r			S_u, a_r, d_f, S_r		
RMSE	75.18	119.023	91.723	74.52	86.52	78.61
MAE	62.75	98.70	74.41	51.036	86.524	55.426
RAE	0.227	0.353	0.268	0.185	0.231	0.199
RRSE	0.235	0.3759	0.286	0.232	0.273	0.245
R^2	0.945	0.940	0.9217	0.946	0.9453	0.942

Table 5. Comparison of the optimal GEP model with previously proposed models for predicting aggregate piers bearing capacity.

Models	References	Input Parameter	Statistical Parameter		
			R^2	MAE	RMSE
			All	All	All
MLR	[13]	S_u, a_r, d_f, S_r	0.92	77.77	93.08
MNR	[29]	S_u, a_r, d_f, S_r	0.93	61.4	82.74
DNN	[29]	S_u, a_r, d_f, S_r	0.92	62.1	NA
MLR	[28]	$S_u, a_r, d_f, S_r, B_f, d_p, l_p$	0.901	79.23	97.77
SVM	[28]	$S_u, a_r, d_f, S_r, B_f, d_p, l_p$	0.88	99.47	124.72
RFR	[28]	$S_u, a_r, d_f, S_r, B_f, d_p, l_p$	0.98	39.83	51.9
ANN	[28]	$S_u, a_r, d_f, S_r, B_f, d_p, l_p$	0.89	68.13	102.2
This Study (GEP4)	This Study (GEP4)	S_u, a_r, d_f, S_r	0.942	55.42	78.61

8. Conclusions

In this study, the gene expression programming was used to estimate the bearing capacity of the aggregate piers reinforced clay soils. The dataset used in this research, despite its lack of comprehensiveness, is the most complete dataset that compiled till now to model the bearing capacity of aggregate piers. If the number of data points for modelling is small, fewer complex models should be employed. Also, the number of input variables should be reduced as much as possible. In this study, the GEP method is used, leading to the construction of simpler non-linear regression models compared to the common machine learning methods (e.g., ANN, SVM, and RFR).

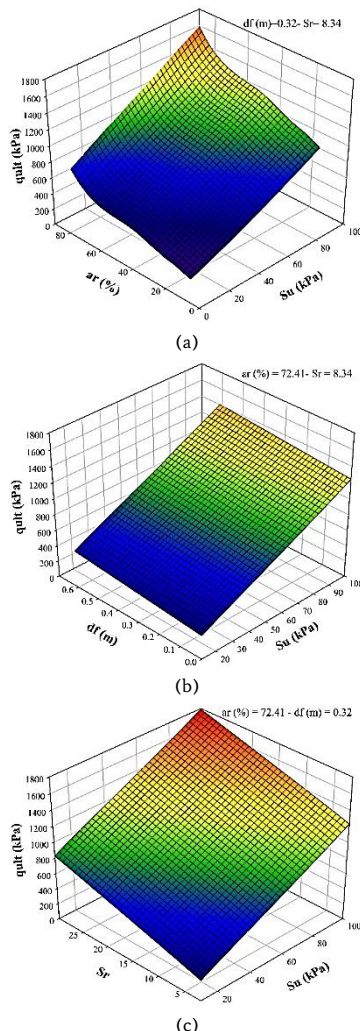
The results of this study showed that the bearing capacity of clay soils reinforced with aggregate piers is mostly affected by the undrained shear strength of soil (S_u), area replacement ratio (a_r), slenderness ratio (S_r), and embedment depth (d_f). Since the importance of two parameters, S_u and a_r , on the bearing capacity is much higher, another GEP model (GEP2) was also built using only these two input variables, which also has a good accuracy.

The R^2 and RMSE values for the GEP4 model (four input variables) were 0.942 and 78.61, respectively. The R^2 and RMSE values for the GEP2 model were 0.921 and 91.723, respectively, which confirms that the GEP4 model is more accurate compared to the GEP2 model. Comparing the MAE and coefficient of determination of the optimal GEP model with the previously proposed models showed that the GEP4 model presented in this study had a superior performance regarding the evaluation of both the number of input parameters and accuracy.

The sensitivity analysis demonstrated that the undrained shear strength of soil (S_u), replacement ratio (a_r), slenderness ratio (S_r), and embedment depth (d_f) had the highest contribution to the bearing capacity, respectively. The parametric analysis also showed that increasing the undrained shear strength of soil (S_u), replacement ratio (a_r), slenderness ratio (S_r), and embedment depth (d_f) led to an increase in the bearing capacity of the aggregate piers reinforced clay, which aligns with the experimental results.

Declaration of Interest Statement

The authors confirm that there are no known conflicts of interest associated with this publication, and there has been no significant financial support for this work that could have influenced its outcome.

**Figure 14.** Parametric analysis for the GEP4 model.

REFERENCES

- [1]. Nicholson PG (2014) Soil improvement and ground modification methods. Butterworth-Heinemann
- [2]. Han J (2015) Principles and practice of ground improvement. John Wiley & Sons
- [3]. Shahu JT, Reddy YR (2011) Clayey soil reinforced with stone column group: model tests and analyses. *Journal of Geotechnical and Geoenvironmental Engineering* 137:1265–1274
- [4]. Yoo C, Lee D (2012) Performance of geogrid-encased stone columns in soft ground: full-scale load tests. *Geosynth Int* 19:480–490
- [5]. Hasan M, Samadhiya NK (2017) Performance of geosynthetic-reinforced granular piles in soft clays: model tests and numerical analysis. *Computers and Geotechnic* 87:178–187
- [6]. Mehrannia N, Nazariafshar J, Kalantary F (2018) Experimental investigation on the bearing capacity of stone columns with granular blankets. *Geotechnical and Geological Engineering* 36:209–222
- [7]. Bunawan AR, Momeni E, Armaghani DJ, Rashid ASA (2018) Experimental and intelligent techniques to estimate bearing capacity of cohesive soft soils reinforced with soil-cement columns. *Measurement* 124:529–538
- [8]. Coldwell E, Khosravi M, Zaregarizi S, et al (2020) Stability analysis of an embankment supported by spatially variable soil-cement columns. In: *Geo-Congress 2020: Foundations, Soil Improvement, and Erosion*. American Society of Civil Engineers Reston, VA, pp 507–515
- [9]. Dehghanbanadaki A, Motamedi S, Ahmad K (2020) FEM-based modelling of stabilized fibrous peat by end-bearing cement deep mixing columns. *Geomechanics and Engineering* 20:75–86
- [10]. Phutthananon C, Jongpradist P, Jongpradist P, et al (2020) Parametric analysis and optimization of T-shaped and conventional deep cement mixing column-supported embankments. *Computers and Geotechnic* 122:103555. <https://doi.org/10.1016/j.compgeo.2020.103555>
- [11]. Vibhoosha MP, Bhasi A, Nayak S (2020) Effect of Geosynthetic Stiffness on the Behaviour of Encased Stone Columns Installed in Lithomargic Clay. In: Prashant A, Sachan A, Desai CS (eds) *Advances in Computer Methods and Geomechanics*. Springer Singapore, Singapore, pp 197–207
- [12]. Waichita S, Jongpradist P, Schweiger HF (2020) Numerical and experimental investigation of failure of a DCM-wall considering softening behaviour. *Computer and Geotechnic* 119:103380. <https://doi.org/10.1016/j.compgeo.2019.103380>
- [13]. Stuedlein AW, Holtz RD (2013) Bearing capacity of spread footings on aggregate pier reinforced clay. *Journal of geotechnical and geoenvironmental engineering* 139:49–58
- [14]. Ashour S, Ghataora G, Jefferson I (2022) Behaviour of Model Stone Column Subjected to Cyclic Loading. *Transportation Geotechnics* 35:100777. <https://doi.org/10.1016/j.trgeo.2022.100777>
- [15]. Ghanti R, Kashliwal A (2008) Ground Improvement Techniques—with a focussed study on stone columns. Dura Build Care PVT LTD Retrieved on January 30:2013
- [16]. Greenwood DA (1970) Mechanical improvement of soils below ground surface. In: *Inst Civil Engineers Proc, London/UK*. pp 11–22
- [17]. Vesić AS (1972) Expansion of cavities in infinite soil mass. *Journal of the Soil Mechanics and Foundations Division* 98:265–290
- [18]. Hughes JMO, Withers NJ, Greenwood DA (1975) A field trial of the reinforcing effect of a stone column in soil. *Geotechnique* 25:31–44
- [19]. Brauns J (1978) Initial bearing capacity of stone columns and sand piles. In: *Int. Symp. on Soil Reinforcing and Stabilizing Techniques in Engineering Practice*. pp 497–512
- [20]. Barksdale RD, Bachus RC (1983) Design and construction of stone columns. Turner-Fairbank Highway Research Center
- [21]. Xin T, Minghua Z, Wei C (2018) Numerical Simulation of a Single Stone Column in Soft Clay Using the Discrete-Element Method. *International Journal of Geomechanics* 18:04018176. [https://doi.org/10.1061/\(ASCE\)GM.1943-5622.0001308](https://doi.org/10.1061/(ASCE)GM.1943-5622.0001308)
- [22]. Xin T, Minghua Z, Zhengbo H, Longjian F (2020) Failure Process of a Single Stone Column in Soft Soil beneath Rigid Loading: Numerical Study. *International Journal of Geomechanics* 20:04020130. [https://doi.org/10.1061/\(ASCE\)GM.1943-5622.0001776](https://doi.org/10.1061/(ASCE)GM.1943-5622.0001776)
- [23]. Mitchell JK (1981) Soil improvement-state of the art report. In: *Proc., 11th Int. Conference. on SMFE*. pp 509–565
- [24]. Bergado DT, Lam FL (1987) Full scale load test of granular piles with different densities and different proportions of gravel and sand on soft Bangkok clay. *Soils and foundations* 27:86–93
- [25]. Alkhorshid NR, Araujo GLS, Palmeira EM, Zornberg JG (2019) Large-scale load capacity tests on a geosynthetic encased column. *Geotextiles and Geomembranes* 47:632–641. <https://doi.org/10.1016/j.geotextmem.2019.103458>
- [26]. Bazzazian Bonab S, Lajevardi SH, Saba HR, et al (2020) Experimental studies on single reinforced stone columns with various positions of geotextile. *Innovative Infrastructure Solutions* 5:98. <https://doi.org/10.1007/s41062-020-00349-0>
- [27]. Ghanizadeh AR, Ghanizadeh A, Asteris PG, et al (2023) Developing bearing capacity model for geogrid-reinforced stone columns improved soft clay utilizing MARS-EBS hybrid method. *Transportation Geotechnics* 38:100906. <https://doi.org/10.1016/j.trgeo.2022.100906>
- [28]. Dadhich S, Sharma JK, Madhira M (2021) Prediction of ultimate bearing capacity of aggregate pier reinforced clay using machine learning. *International Journal of Geosynthetics and Ground Engineering* 7:1–16
- [29]. Bong T, Kim S-R, Kim B-I (2020) Prediction of ultimate bearing capacity of aggregate pier reinforced clay using multiple regression analysis and deep learning. *Applied Sciences* 10:4580
- [30]. Kim B-I, Lee S-H (2005) Comparison of bearing capacity characteristics of sand and gravel compaction pile treated ground. *KSCSE Journal of Civil Engineering* 9:197–203
- [31]. Ali K, Shahu JT, Sharma KG (2010) Behaviour of reinforced stone columns in soft soils: an experimental study. In: *Indian geotechnical conference*. pp 620–628
- [32]. Black JA, Sivakumar V, Bell A (2011) The settlement performance of stone column foundations. *Géotechnique* 61:909–922
- [33]. Fattah MY, Al-Neami MA, Al-Suhaily AS (2017) Estimation of bearing capacity of floating group of stone columns. *Engineering science and technology, an international journal* 20:1166–1172
- [34]. Ambily AP, Gandhi SR (2007) Behavior of stone columns based on experimental and FEM analysis. *Journal of geotechnical and geoenvironmental engineering* 133:405–415
- [35]. Hanna AM, Etezzad M, Ayadat T (2013) Mode of failure of a group of stone columns in soft soil. *International Journal of*

Geomechanics 13:87–96

- [36]. Mohanty P, Samanta M (2015) Experimental and numerical studies on response of the stone column in layered soil. *International Journal of Geosynthetics and Ground Engineering* 1:1–14
- [37]. Algin HM, Gumus V (2018) 3D fe analysis on settlement of footing supported with rammed aggregate pier group. *International Journal of Geomechanics* 18:1–18
- [38.]. Etezad M, Hanna AM, Ayadat T (2015) Bearing capacity of a group of stone columns in soft soil. *International Journal of Geomechanics* 15:1–15
- [39]. Naseer S, Sarfraz Faiz M, Iqbal S, Jamil SM (2019) Laboratory and numerical based analysis of floating sand columns in clayey soil. *International Journal of Geo-Engineering* 10:10. <https://doi.org/10.1186/s40703-019-0106-6>
- [40]. Mansourian A, Ghanizadeh AR, Golchin B (2018) Modeling of resilient modulus of asphalt concrete containing reclaimed asphalt pavement using feed-forward and generalized regression neural networks. *Journal of Rehabilitation in Civil Engineering* 6:132–147
- [41]. Kellouche Y, Boukhatem B, Ghrici M, Tagnit-Hamou A (2019) Exploring the major factors affecting fly-ash concrete carbonation using artificial neural network. *Neural Computational Application* 31:969–988. <https://doi.org/10.1007/s00521-017-3052-2>
- [42]. Ma CK, Lee YH, Awang AZ, et al (2019) Artificial neural network models for FRP-repaired concrete subjected to pre-damaged effects. *Neural Computational Application* 31:711–717. <https://doi.org/10.1007/s00521-017-3104-7>
- [43]. Nasrollahzadeh K, Afzali S (2019) Fuzzy logic model for pullout capacity of near-surface-mounted FRP reinforcement bonded to concrete. *Neural Computational Application* 31:7837–7865. <https://doi.org/10.1007/s00521-018-3590-2>
- [44]. Su H, Fu Z, Wen Z (2019) SFPSO algorithm-based multi-scale progressive inversion identification for structural damage in concrete cut-off wall of embankment dam. *Applied Soft Computing* 84:105679. <https://doi.org/10.1016/j.asoc.2019.105679>
- [45]. Xue W, Xu Z, Wang H, Ren Z (2019) Hazard assessment of landslide dams using the evidential reasoning algorithm with multi-scale hesitant fuzzy linguistic information. *Applied Soft Computing* 79:74–86. <https://doi.org/10.1016/j.asoc.2019.03.032>
- [46]. Ghanizadeh AR, Heidarabadi N, Jalali F (2020) Artificial neural network back-calculation of flexible pavements with sensitivity analysis using Garson's and connection weights algorithms. *Innovative Infrastructure Solutions* 5:63. <https://doi.org/10.1007/s41062-020-00312-z>
- [47]. Jebur AA, Atherton W, al Khaddar RM, Loffill E (2021) Artificial neural network (ANN) approach for modelling of pile settlement of open-ended steel piles subjected to compression load. *European Journal of Environmental and Civil Engineering* 25:429–451. <https://doi.org/10.1080/19648189.2018.1531269>
- [48]. Ghanizadeh AR, Ziaee A, Khatami SMH, Fakharian P (2022) Predicting Resilient Modulus of Clayey Subgrade Soils by Means of Cone Penetration Test Results and Back-Propagation Artificial Neural Network. *Journal of Rehabilitation in Civil Engineering* 10:146–162
- [49]. Goh ATC (1995) Empirical design in geotechnics using neural networks. *Geotechnique* 45:709–714
- [50]. Chan WT, Chow YK, Liu LF (1995) Neural network: an alternative to pile driving formulas. *Computers and Geotechnic* 17:135–156
- [51]. Das SK, Basudhar PK (2006) Undrained lateral load capacity of piles in clay using artificial neural network. *Computers and Geotechnic* 33:454–459
- [52]. Das M, Dey AK (2018) Prediction of Bearing Capacity of Stone Columns Placed in Soft Clay Using ANN Model. *Geotechnical and Geological Engineering* 36:1845–1861. <https://doi.org/10.1007/s10706-017-0436-0>
- [53]. Dey AK, Debnath P (2020) Empirical approach for bearing capacity prediction of geogrid-reinforced sand over vertically encased stone columns floating in soft clay using support vector regression. *Neural Computational Applied* 32:6055–6074. <https://doi.org/10.1007/s00521-019-04092-1>
- [54]. Ardakani A, Dinarvand R, Namaei A (2020) Ultimate Shear Resistance of Silty Sands Improved by Stone Columns Estimation Using Neural Network and Imperialist Competitive Algorithm. *Geotechnical and Geological Engineering* 38:1485–1496. <https://doi.org/10.1007/s10706-019-01104-8>
- [55]. Dehghanbanadaki A (2021) Intelligent modelling and design of soft soil improved with floating column-like elements as a road subgrade. *Transportation Geotechnics* 26:100428. <https://doi.org/https://doi.org/10.1016/j.tge.2020.100428>
- [56]. Das M, Dey AK (2022) Prediction of Bearing Capacity of Stone Columns Using Type-2 Fuzzy Logic. In: Das BB, Hettiarachchi H, Sahu PK, Nanda S (eds) *Recent Developments in Sustainable Infrastructure (ICRDSI-2020)—GEO-TRA-ENV-WRM: Conference Proceedings from ICRDSI-2020 Vol. 2*. Springer Singapore, Singapore, pp 413–437
- [57]. Ferreira C (2001) Gene expression programming: a new adaptive algorithm for solving problems. *arXiv preprint cs/0102027*
- [58]. Ferreira C (2002) Gene expression programming in problem solving. In: *Soft computing and industry*. Springer, pp 635–653
- [59]. Shahmansouri AA, Bengar HA, Ghanbari S (2020) Compressive strength prediction of eco-efficient GGBS-based geopolymer concrete using GEP method. *Journal of Building Engineering* 31:101326
- [60]. Mahdinia S, Eskandari-Naddaf H, Shadnia R (2019) Effect of cement strength class on the prediction of compressive strength of cement mortar using GEP method. *Construction and Building Materials* 198:27–41
- [61]. Javed MF, Amin MN, Shah MI, et al (2020) Applications of Gene Expression Programming and Regression Techniques for Estimating Compressive Strength of Bagasse Ash based Concrete. *Crystals (Basel)* 10:737. <https://doi.org/10.3390/cryst10090737>
- [62]. Alinezhadi M, Mousavi SF, Hosseini Kh (2021) Comparison of Gene Expression Programming (GEP) and Parametric and Non-parametric Regression Methods in the Prediction of the Mean Daily Discharge of Karun River (A case Study: Mollasani Hydrometric Station). *JSTNAR* 25:43–62. <https://doi.org/10.47176/jwss.25.1.1012>
- [63]. Ganguly S, Datta S, Chakraborti N (2009) Genetic algorithm-based search on the role of variables in the work hardening process of multiphase steels. *Computational Material Science* 45:158–166
- [64]. Bhargava S, Dulikravich GS, Murty GS, et al (2011) Stress corrosion cracking resistant aluminum alloys: Optimizing concentrations of alloying elements and tempering. *Materials and Manufacturing Processes* 26:363–374
- [65]. Shahmansouri AA, Bengar HA, Jahani E (2019) Predicting compressive strength and electrical resistivity of eco-friendly concrete containing natural zeolite via GEP algorithm. *Construction and Building Material* 229:1–18

- [66]. Naderpour H, Nagai K, Fakharian P, Haji M (2019) Innovative models for prediction of compressive strength of FRP-confined circular reinforced concrete columns using soft computing methods. *Composite Structure* 215:69–84
- [67]. Martin JP (2018) A Full-Scale Experimental Investigation of the Bearing Performance of Aggregate Pier-Supported Shallow Foundations
- [68]. Bergado DT, Lam FL (1987) Full scale load test of granular piles with different densities and different proportions of gravel and sand on soft Bangkok clay. *Soils and foundations* 27:86–93
- [69]. Baumann V, Bauer GEA (1974) The performance of foundations on various soils stabilized by the vibro-compaction method. *Canadian Geotechnical Journal* 11:509–530
- [70]. Stuedlein AW, Holtz RD (2012) Analysis of footing load tests on aggregate pier reinforced clay. *Journal of Geotechnical and Geoenvironmental Engineering* 138:1091–1103
- [71]. Greenwood DA (1975) Vibroflotation: rationale for design and practice. *Methods of treatment of unstable ground* 189–209
- [72]. Hughes JMO, Withers NJ, Greenwood DA (1975) A field trial of the reinforcing effect of a stone column in soil. *Geotechnique* 25:31–44
- [73]. Han J, Ye S (1991) Field tests of soft clay stabilized by stone columns in coastal areas of China. In: *Proc., 4th Int. Deep Foundations Institute Conf.* pp 243–248
- [74]. Lillis C, Lutenege AJ, Adams M (2004) Compression and uplift of rammed aggregate piers in clay. In: *GeoSupport 2004: Drilled Shafts, Micropiling, Deep Mixing, Remedial Methods, and Specialty Foundation Systems.* pp 497–507
- [75]. White DJ, Pham HT v, Hoevelkamp KK (2007) Support mechanisms of rammed aggregate piers. I: Experimental results. *Journal of Geotechnical and Geoenvironmental Engineering* 133:1503–1511
- [76]. Khan K, Jalal FE, Iqbal M, et al (2022) Predictive Modeling of Compression Strength of Waste PET/SCM Blended Cementitious Grout Using Gene Expression Programming. *Materials* 15:3077
- [77]. Chen X-Y, Chau K-W (2019) Uncertainty analysis on hybrid double feedforward neural network model for sediment load estimation with LUBE method. *Water Resources Management* 33:3563–3577
- [78]. Gandomi AH, Yun GJ, Alavi AH (2013) An evolutionary approach for modeling of shear strength of RC deep beams. *Materials and Structure* 46:2109–2119
- [79]. Javed MF, Amin MN, Shah MI, et al (2020) Applications of gene expression programming and regression techniques for estimating compressive strength of bagasse ash based concrete. *Crystals (Basel)* 10:737
- [80]. Shah MI, Javed MF, Abunama T (2021) Proposed formulation of surface water quality and modelling using gene expression, machine learning, and regression techniques. *Environmental Science and Pollution Research* 28:13202–13220
- [81]. Azim I, Yang J, Javed MF, et al (2020) Prediction model for compressive arch action capacity of RC frame structures under column removal scenario using gene expression programming. In: *Structures.* Elsevier, pp 212–228
- [82]. Iqbal MF, Liu Q, Azim I, et al (2020) Prediction of mechanical properties of green concrete incorporating waste foundry sand based on gene expression programming. *J Hazardous Materials* 384:121322
- [83]. Alavi AH, Gandomi AH, Nejad HC, et al (2013) Design equations for prediction of pressuremeter soil deformation moduli utilizing expression programming systems. *Neural Computational Applied* 23:1771–1786. <https://doi.org/10.1007/s00521-012-1144-6>
- [84]. Emamgolizadeh S, Bateni SM, Shahsavani D, et al (2015) Estimation of soil cation exchange capacity using Genetic Expression Programming (GEP) and Multivariate Adaptive Regression Splines (MARS). *Journal of Hydrology (Amst)* 529:1590–1600. <https://doi.org/10.1016/j.jhydrol.2015.08.025>